

FACTA UNIVERSITATIS

Series: **Mechanical Engineering** Vol. 15, N° 2, 2017, pp. 295 - 306

DOI: 10.22190/FUME170503007D

Original scientific paper

SIMULATION OF FRICTIONAL DISSIPATION UNDER BIAXIAL TANGENTIAL LOADING WITH THE METHOD OF DIMENSIONALITY REDUCTION

UDC 531.4

Andrey V. Dimaki¹, Roman Pohrt², Valentin L. Popov^{2,3,4}¹Institute of Strength Physics and Materials Science SB RAS, Tomsk, Russia²Berlin University of Technology, Germany³National Research Tomsk Polytechnic University, Russia⁴National research Tomsk State University, Russia

Abstract. *The paper is concerned with the contact between the elastic bodies subjected to a constant normal load and a varying tangential loading in two directions of the contact plane. For uni-axial in-plane loading, the Cattaneo-Mindlin superposition principle can be applied even if the normal load is not constant but varies as well. However, this is generally not the case if the contact is periodically loaded in two perpendicular in-plane directions. The applicability of the Cattaneo-Mindlin superposition principle guarantees the applicability of the method of dimensionality reduction (MDR) which in the case of a uni-axial in-plane loading has the same accuracy as the Cattaneo-Mindlin theory. In the present paper we investigate whether it is possible to generalize the procedure used in the MDR for bi-axial in-plane loading. By comparison of the MDR-results with a complete three-dimensional numeric solution, we arrive at the conclusion that the exact mapping is not possible. However, the inaccuracy of the MDR solution is on the same order of magnitude as the inaccuracy of the Cattaneo-Mindlin theory itself. This means that the MDR can be also used as a good approximation for bi-axial in-plane loading.*

Key Words: *Friction, Dissipation, Tangential Contact, Biaxial In-plane Loading, Circular Loading, Cattaneo, Mindlin, MDR*

1. INTRODUCTION

Friction is a dissipative process transforming mechanical energy into heat and material changes of the contacting partners. The energy dissipation may be connected with material dissipation (wear) [1] or utilized for structural damping [2]. Studying both wear and

Received May 03, 2017 / Accepted June 20, 2017**Corresponding author:** Andrey V. Dimaki

Institute of Strength Physics and Materials Science SB RAS, Akademicheskii av. 2/4, 634055 Tomsk, Russia

E-mail: dav@ispms.tsc.ru

damping requires the solution of a tangential contact problem. The simplest case of a tangential loading is an increasing uni-axial tangential loading at a constant normal force. This problem has been solved first by Cattaneo [3] and later independently by Mindlin [4]. They have shown that a tangential stress distribution can be represented as a superposition of two solutions for the normal contact problem of the same geometry, only multiplied with the coefficient of friction. This reduction to the normal contact problem is exactly the feature which allows the application of the method of dimensionality reduction (MDR) [5], (see also Chapter 5 devoted to tangential contact in [6]). However, Cattaneo and Mindlin have not noticed a small inconsistency in their solution. In their theory, it is assumed that the frictional stresses in the slip domain are all directed in the direction of the applied tangential force. With the exception of the unrealistic case where both the contacting materials have Poisson ratio zero, this assumption violates the condition that at every position in the slip domain, the slip is directed in the direction opposing the tangential stresses. The reason for this is the presence of an additional slip motion perpendicular to the direction of the applied force. This was first pointed out by Johnson [7] who showed that the maximum inclination of slip angle is on the order of magnitude $v/(4-v)$ which is equal to 0.09 for $v=1/3$ and 0.14 for $v=1/2$. He concluded that the error is not large and that the Cattaneo-Mindlin solution is a good approximation. Later comparisons with numerical solutions have shown that the above mentioned inconsistency may have an important influence on the distribution of wear but has almost no impact on the macroscopic force-displacement relations [8]. A detailed analysis can be found also in [9].

In the present paper we consider a more complicated problem of bi-axial oscillating loading (superimposed loading in two in-plane directions). The aim of the paper is twofold: on one hand, we are interested in a better understanding of the energy dissipation in bi-axially loaded contacts; on the other hand, we would like to check the applicability of the dimensionality reduction method to this class of problems. At present, there are only a few numerical studies providing the dependencies of dissipated friction energy on the parameters of loading [10]. The applicability of the MDR would provide a simple tool for simulating arbitrary loading histories with applications in the dynamics of structures with frictional contacts.

2. ENERGY DISSIPATION IN A SINGLE-POINT CONTACT FOR CIRCULAR MOVEMENT

Let us start by considering a single isotropic linearly elastic massless element which can deform in normal direction as well as in two tangential directions. We will call this element a “spring”. The spring should have out-of-plane stiffness k_z and isotropic in-plane stiffness $k_x=k_y$. It is first pressed against a rigid half-plane with a normal force F_z and then moved in the direction of the x -axis. We will assume that at the immediate contact point between the spring and the substrate, there is friction characterized by a constant coefficient of friction μ . When the free end of the spring is moved horizontally, it first deforms elastically until the in-plane displacement achieves the critical value

$$l_0 = \mu F_z / k_x. \quad (1)$$

After this, the lower contact point starts sliding and the force remains constant.

If the spring is moved on a circle with radius $R < l_0$, then it remains in the stick state at any time. However, if the radius of movement exceeds critical value, $R \geq l_0$, the contact

point will slip. In the stationary state, it will move in a circle with a smaller radius r_c , while the in-plane displacement of the spring remains constant and equal to l_0 . The frictional force is assumed to be opposite to the elastic force and at the same time it has to be directed opposite to the velocity vector. Therefore, the contact point between the spring and the half-plane will move in the direction of the elastic displacement. On the other hand, this velocity will be directed tangentially to the inner circle with radius r_c , which means that the elastic displacement of the spring is directed tangentially to this circle, as shown in Fig. 1. The dissipation power is then obviously given by the equation

$$\dot{W} = v_{\text{macro}} \cdot \mu F_z \cdot \cos \theta = v_{\text{macro}} \mu F_z \sqrt{1 - (l_0 / R)^2}, \quad (2)$$

where v_{macro} is the absolute velocity of the spring motion. For one cycle of motion with radius $R > l_0$ the value of the dissipated energy is

$$W = \dot{W} \Delta t_{\text{cycle}} = 2\pi R \mu F_z \sqrt{1 - (l_0 / R)^2}, \quad (3)$$

where Δt_{cycle} is the time needed to perform one cycle of circular motion. If the initial position of the spring does not correspond to the stationary one, it moves on a spiral asymptotically approaching the circle with radius r_c as shown in Fig. 1b.

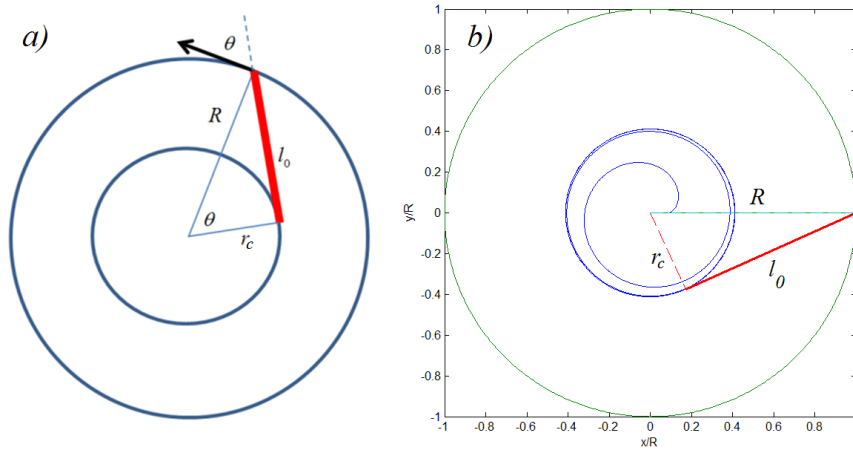


Fig. 1 a) The scheme of a circular motion of a single spring; b) The results of the numerical simulation: the evolution of the trajectory of a single spring during a circular motion

3. ENERGY DISSIPATION IN A CURVED CONTACT FOR CIRCULAR MOVEMENT

Generally, a non-conforming contact between elastic solids cannot be modeled with a single spring. In the case of uni-axial in-plane loading, the contact problem can be reduced to a contact of a rigid plane profile with a series of independent springs. This method is known as the method of dimensionality reduction [5, 6, 11]. It replaces a contact between two continuum bodies with an ensemble of independent one-spring problems and thus reduces the general contact problem to the above one-spring problem (see Fig. 2).

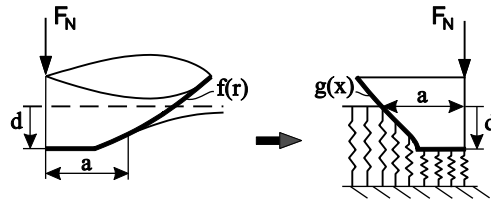


Fig. 2 Mapping of a three-dimensional contact into one-dimensional one

If the MDR-procedure was applicable to the bi-axial in-plane loading, then we could compute the energy dissipation rate just by summing Eq. (2) over all effective springs of the MDR-model. Let us *assume* at this point that this is indeed possible and calculate the dissipation in a circularly moving and curved contact. Later we will check and discuss the accuracy of this procedure.

We consider the movement of a parabolic indenter having the shape $z=f(r)=r^2/(2r_0)$. According to the MDR-rules [5, 6], in the equivalent MDR model it is to be replaced by the plane profile

$$g(x) = |x| \int_0^{|x|} \frac{f'(r) dr}{\sqrt{x^2 - r^2}} = \frac{x^2}{r_0}. \quad (4)$$

This profile is brought into contact with an elastic foundation consisting of independent springs, each spring having normal stiffness Δk_z and equal tangential stiffnesses Δk_x and Δk_y for the displacements along the x -axis and y -axis (not shown in Fig. 2) which are defined according to the rules

$$\Delta k_z = E^* \Delta x, \quad \Delta k_x = \Delta k_y = G^* \Delta x, \quad (5)$$

where

$$\frac{1}{E^*} = \frac{1-\nu_1^2}{E_1} + \frac{1-\nu_2^2}{E_2} \quad \text{and} \quad \frac{1}{G^*} = \frac{(2-\nu_1)}{4G_1} + \frac{(2-\nu_2)}{4G_2}, \quad (6)$$

with E_1 and E_2 being the Young's moduli, G_1 and G_2 the shear moduli and ν_1 and ν_2 the Poisson's ratios of the contacting bodies. Further, throughout the paper, we assume that the contacting materials satisfy the condition of "elastic similarity"

$$\frac{1-2\nu_1}{G_1} = \frac{1-2\nu_2}{G_2}, \quad (7)$$

which guarantees the decoupling of normal and tangential contact problems [12].

If the indentation depth is d , then the vertical displacement of an individual spring at position x is given by

$$u_{z,1D}(x) = d - g(x) \quad (8)$$

and the normal force of a single spring equals to

$$\Delta F_z(x) = \Delta k_z (d - g(x)) = E^* \Delta x (d - g(x)). \quad (9)$$

The dissipation power in one spring at the position x is given by Eq. (2) which we rewrite here as

$$\Delta \dot{W} = \mu \Delta F_z \sqrt{1 - \left(\mu \frac{\Delta F_z}{R \Delta k_x} \right)^2} = v_{\text{macro}} \mu E^* \Delta x (d - g(x)) \sqrt{1 - \left(\mu \frac{E^*}{G^*} \frac{(d - g(x))}{R} \right)^2}. \quad (10)$$

Let us assume that we have a situation with partial slip. Radius c of the stick region is determined by the condition

$$d - g(c) = \frac{1}{\mu} R \frac{G^*}{E^*} \quad (11)$$

whence

$$\frac{c^2}{r_0} = d - \frac{1}{\mu} R \frac{G^*}{E^*}. \quad (12)$$

The whole dissipation power is thus equal to

$$\dot{W} = \frac{2v_{\text{macro}} \mu E^*}{r_0} \int_c^a (a^2 - x^2) \sqrt{1 - \left(\frac{a^2 - x^2}{a^2 - c^2} \right)^2} dx, \quad (13)$$

where $a = \sqrt{r_0 d}$ is the contact radius. Evaluation of the integral yields

$$\dot{W} = \frac{3}{2} v_{\text{macro}} \mu F_z \Phi(\tilde{c}), \quad (14)$$

where

$$\Phi(\tilde{c}) = \int_{\tilde{c}}^1 (1 - \xi^2) \sqrt{1 - \left(\frac{1 - \xi^2}{1 - \tilde{c}^2} \right)^2} d\xi \quad (15)$$

with $\tilde{c} = c/a$. Function $\Phi(\tilde{c})$ is shown in Fig. 3. From (14) we see that the energy dissipation power is given by the formally calculated "nominal power" $v_{\text{macro}} \mu F_z$ multiplied with function $\frac{3}{2} \Phi(\tilde{c})$, which only depends on the reduced radius of the stick area.

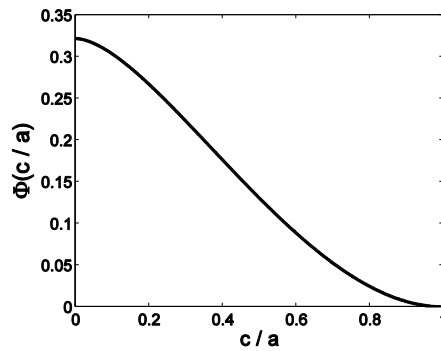


Fig. 3 Dependence $\Phi(\tilde{c})$

4. CALCULATION OF STRESSES IN THE FRAMEWORK OF MDR

The above MDR-solution is based on the Coulomb criterion for sticking and sliding for the springs of the effective one-dimensional elastic foundation. This MDR model gives the correct solution to the three-dimensional problem only if the conditions for sticking and sliding are fulfilled also for in-plane stresses in relation with normal stresses in the initial (truly three-dimensional) problem. We thus begin our analysis by checking the fulfillment of the sticking conditions and go later to an additional validation by comparison with results of direct 3D simulation given in [10].

According to the MDR rules, the distribution of normal pressure p in the three-dimensional problem may be calculated using the following integral transformation [11]:

$$p(r) = -\frac{1}{\pi} \int_r^\infty \frac{q'_z(x)}{\sqrt{x^2 - r^2}} dx, \quad (16)$$

where $q_z(x) = \Delta F_z(x)/\Delta x$ is a linear density of the normal force. A similar transformation is valid for the tangential stress:

$$\tau_x(r) = -\frac{1}{\pi} \int_r^\infty \frac{q'_x(x)}{\sqrt{x^2 - r^2}} dx, \quad (17)$$

where $q_x(x) = \Delta F_x(x)/\Delta x$ is a linear density of the tangential reaction force, respectively. The proof for these rules can be found in Appendix D of Ref. [5]. This proof can be easily generalized to an arbitrary two in-plane dimensions and shows that the transformation (17) can be applied separately to each component of tangential stress, so we can obtain tangential stresses in y-direction similar to Eq. (17):

$$\tau_y(r) = -\frac{1}{\pi} \int_r^\infty \frac{q'_y(x)}{\sqrt{x^2 - r^2}} dx. \quad (18)$$

Thus, for calculating the stress component we have to determine first the linear force densities $q_x(x) = \Delta F_x(x)/\Delta x$ and $q_y(x) = \Delta F_y(x)/\Delta x$.

Let us denote the coordinates of a spring tip as $(u_{x,tip}, u_{y,tip})$ and the coordinates of the upper point of the spring as (u_x, u_y) . Assume that in an iteration step the coordinates of the spring u_x and u_y , are changed by δu_x and δu_y , so that

$$\begin{cases} \tilde{u}_x = u_x + \delta u_x \\ \tilde{u}_y = u_y + \delta u_y \end{cases}. \quad (19)$$

If new coordinates \tilde{u}_x and/or \tilde{u}_y now lie outside a circle having a central point $(u_{x,tip}, u_{y,tip})$ and a radius $l_0(x)$:

$$l_0(x) = \mu \Delta F_z(x) / \Delta k_x, \quad (20)$$

then the spring tip will start to slide in the direction of the tangential reaction force (see Fig. 4) until it reaches the point $(\tilde{u}_{x,tip}, \tilde{u}_{y,tip})$:

$$\sqrt{(\tilde{u}_x - \tilde{u}_{x,tip})^2 + (\tilde{u}_y - \tilde{u}_{y,tip})^2} = l_0(x). \quad (21)$$

In other words, the new equilibrium point lays on the straight line connecting the points $(u_{x,tip}, u_{y,tip})$ and $(\tilde{u}_x, \tilde{u}_y)$, at distance $l_0(x)$ from $(\tilde{u}_x, \tilde{u}_y)$ (see Fig. 4).

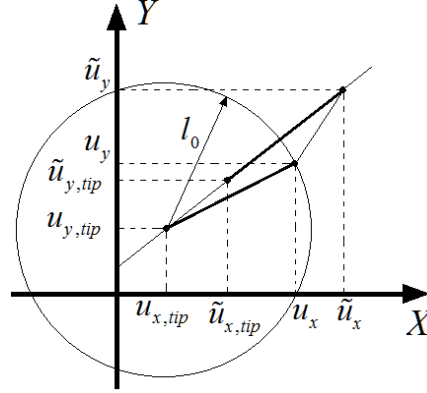


Fig. 4 The slip displacement of a single spring in XY plane under lateral motion

The components of the tangential reaction force of the spring can be found as follows:

$$\begin{cases} \Delta F_x(x) = \Delta k_x(u_x - u_{x,tip}) \\ \Delta F_y(x) = \Delta k_y(u_y - u_{y,tip}) \end{cases} \quad (22)$$

We have studied the frictional energy dissipation for the parabolic indenter with the following fictive parameters: $r_0=1$ m, $E^*=1$ GPa, $d=0.001$ m, $\nu=0.28$, $\mu=0.3$. The indenter was initially moved to the point $(U_{x0}, 0)$ and then subjected to an in-plane harmonic displacement

$$\begin{cases} U_x(t) = U_{x0} \cos(\omega t) \\ U_y(t) = U_{y0} \sin(\omega t) \end{cases} \quad (23)$$

Controlling the tangential reaction forces in Ox and Oy directions, it is possible to introduce the force-dependent governing parameters, following the paper of Ciavarella [10]:

$$Q / \mu F_z \text{ and } R_M = Q_x / Q_y, \quad (24)$$

where

$$Q_x = \max |F_x(t)|, \quad Q_y = \max |F_y(t)|, \quad Q = \sqrt{Q_x^2 + Q_y^2}. \quad (25)$$

Note that the value of Q , defined in Eq. (25), does not correspond to any real tangential force acting on the indenter, but it serves only as a governing parameter in the parametric study of the problem under consideration.

With Eq. (22) we determine linear force densities $q_x(x)=\Delta F_x(x)/\Delta x$ and $q_y(x)=\Delta F_y(x)/\Delta x$. We then calculate the tangential stress components given by Eqs. (17) and (18) and finally the absolute value of the tangential stress:

$$\tau_{MDR}(r) = \sqrt{\tau_x^2(r) + \tau_y^2(r)} \quad (26)$$

The corresponding dependencies are presented in Fig. 5 together with the normal stress distribution multiplied with the coefficient of friction and the formal Mindlin solution with the same radius of stick region (dashed lines in Fig. 5). One can see that the obtained stress distributions do not exactly fulfill the conditions for stick and slip. In most ranges of radii smaller than the stick radius, the tangential stress is smaller than the normal stress multiplied with the coefficient of friction; there is only a small region inside the stick radius with τ too high. Thus the stick condition is fulfilled not exactly but in good approximation. However, for radii moderately larger the stick radius, the tangential stress is higher than the normal stress times the coefficient of friction, which means that the sliding condition is not fulfilled. At even larger radii, the condition that in the sliding region the tangential stress must be equal to normal stress times the coefficient of friction is fulfilled with good accuracy. Thus, the tangential stress distribution has a qualitatively correct shape but it does not exactly match the stick and slip conditions.

The mentioned discrepancy is observed only in a relatively narrow interval of radii. Thus, the integral influence of this error may be moderate. This situation can be compared with the solution by Cattaneo and Mindlin which also has a local error, but the global error in the force-displacement relations is moderate and is generally tolerated.

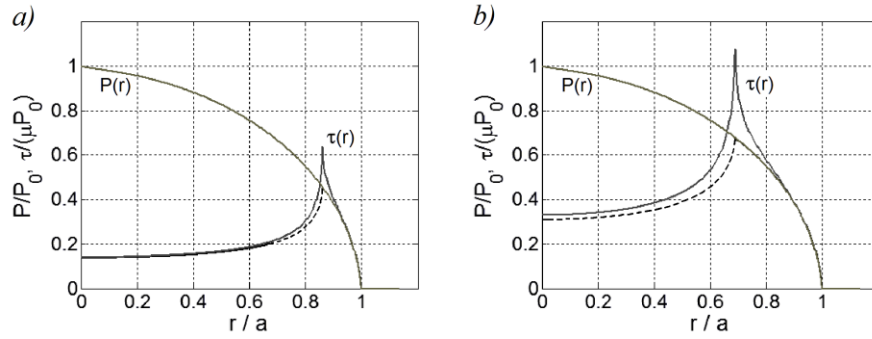


Fig. 5 The distributions of normal pressure and the absolute value of tangential stress. P_0 is the pressure under the axis of the indenter. The dashed line indicates the formal Mindlin solution with the same radius of stick region. $R_M = 1$. a) $Q/\mu F_z = 0.5$; b) $Q/\mu F_z = 0.9$

In order to estimate the possible global error, let us determine the integral discrepancy between the obtained stress distribution and the Cattaneo-Mindlin distribution [3] (which fulfils the stick and slip conditions):

$$\Delta = 100\% \cdot \left| \frac{2\pi \int_0^a \tau_{MDR}(r) r dr - 2\pi \int_0^a \tau_{CM}(r) r dr}{2\pi \int_0^a \tau_{CM}(r) r dr} \right|, \quad (27)$$

where $\tau_{CM}(r)$ corresponds to the Cattaneo-Mindlin solution. This discrepancy is shown in Fig. 6. The integral difference between tangential stresses, predicted by the theory of Cattaneo-Mindlin, and the MDR results, is about two percent for low values of $Q/\mu F_z$ and R_M . This means that the above MDR theory has a good accuracy at least for oscillations with small amplitude comparable to the full slip displacement.

Further, let us compare the results of MDR simulation with the full three-dimensional calculations. The tangential stresses are calculated using MDR as described above for the following set of parameters: $R_M = 1$, $Q = 0.9$, which correspond to the same values as used in Ref. [10]. Comparison of the MDR results with results of full three-dimensional simulations is presented in Fig. 7.

In Fig. 7, on the left hand side, the stress-field simulated by the MDR is presented and so is, on the right hand side, the stress field from the three-dimensional simulation [10]. While both results are in a good qualitative agreement, one can also see some differences. Firstly, the stick radius in the MDR results does not decrease after the start of the in-plane rotation, which can be connected to the application of the tangential displacement instead of tangential forces in 3D simulation. Secondly, the tangential stresses in the stick area in the MDR solution are higher than those in the full 3D calculation. However, the mentioned discrepancies between the MDR results and full 3D calculations are moderate. We can conclude that the MDR can be also used with “engineering accuracy” for contact problems with bi-axial in-plane loading.

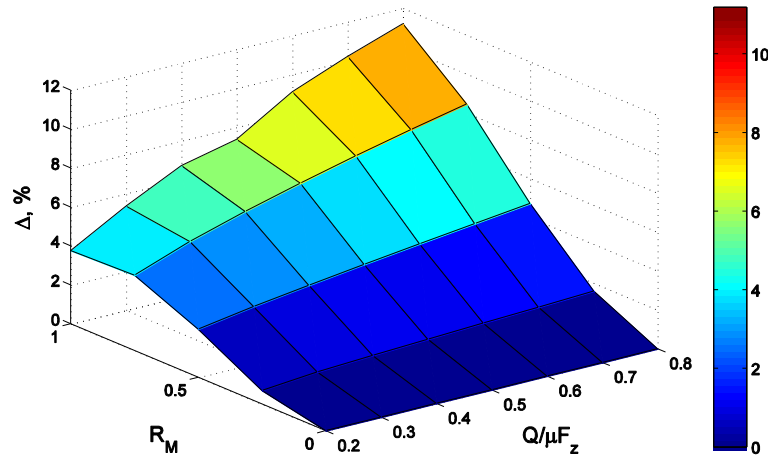


Fig. 6 The integral difference (27) between tangential stresses, predicted by the Cattaneo-Mindlin theory, and the MDR results

5. NUMERICAL SIMULATION OF DISSIPATION UNDER NON-CIRCULAR MOTION

In this paragraph we apply the MDR within its range of accuracy for studying energy dissipation in a contact subject to biaxial tangential loading with different oscillation amplitudes in two perpendicular directions. In order to normalize values of dissipated energy we use the solution of Mindlin [3] for friction energy dissipation during one cycle of a uniaxial tangential loading:

$$W_C = W_{R_M=0} = \frac{9\mu^2 F_z^2}{10a} \frac{2}{G^*} \left\{ 1 - \left(1 - \frac{Q}{\mu F_z} \right)^{5/3} - \frac{5Q}{6\mu F_z} \left[1 + \left(1 - \frac{Q}{\mu F_z} \right)^{2/3} \right] \right\}. \quad (28)$$

In the performed calculations we have varied the governing parameters (24) in a wide range of values. The results of simulation, accompanied with the corresponding results of the full 3D simulations, given in Ref. [10], are shown in Fig. 8a. It can be seen that the MDR results are in a good agreement with the results of the full 3D simulations, except for the curve for $R_M = 1$ which also is in a qualitative agreement but shows distinctive quantitative differences.

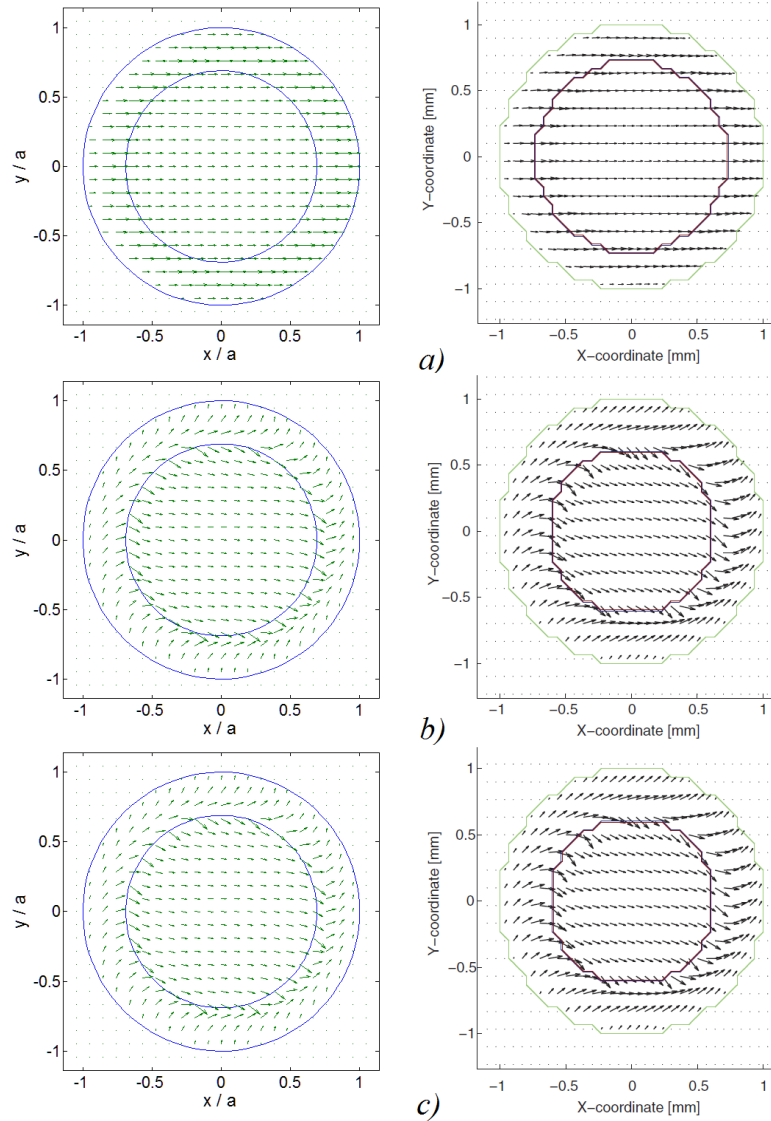


Fig.7 The distributions of tangential stresses in the contact area - the results of the MDR simulation in the left column, the results of the full 3D simulation, from Ref. [10], in the right column: a) after the initial displacement; b) after one revolution; c) after two revolutions; $R_M=1$, $Q=0.9$. The inner circle indicates the stick area

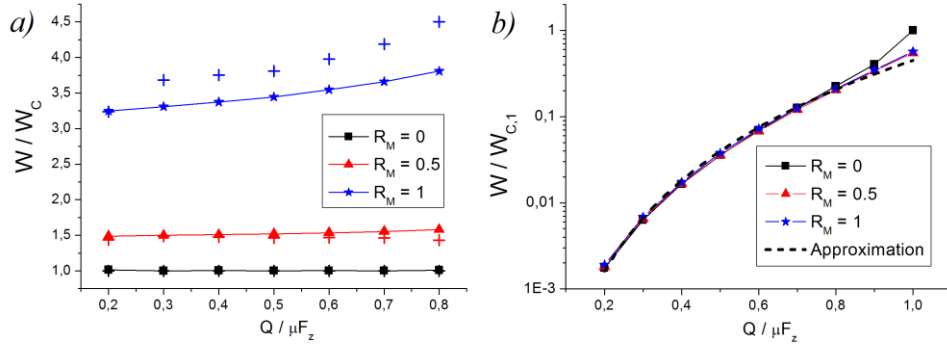


Fig. 8 a) The normalized dependencies of the energy, dissipated during one cycle of the circular motion, compared with the data from Ref. [10] (indicated by the crosses); b) The normalized dependencies of the energy, dissipated during one cycle of the circular motion, reduced into the universal curve. The normalizing factor $W_{1,C}$ is given by Eq. (29)

We have found that for various values of R_M , the dependencies of W on $Q/\mu F_z$ can be reduced to a universal curve (Fig. 8b). The results are normalized to the value of the energy $W_{1,C}$ dissipated during one cycle of uniaxial loading with $Q/\mu F_z=1$:

$$W_{1,C} = W_{R_M=0, Q=\mu F_z} = \frac{3\mu^2 F_z^2}{10aG^*}. \quad (29)$$

The universality of the given curve holds for relatively small amplitudes of oscillations. When the amplitude of oscillations becomes comparable with the value of amplitude needed for gross slip transition, the deviations from the universal curve appear (see Fig. 8b). We suggest a power-law approximation of the data shown in Fig. 8b as follows:

$$W = 0.45 W_{1,C} (Q/\mu F_z)^{3.5}, \quad (30)$$

which fits the results of numerical simulations well for $Q/\mu F_z < 0.7$. Note that in Fig. 8b the curve for $R_M = 0$ coincides with the results of Cattaneo and Mindlin.

6. CONCLUSIONS

By analyzing the stick and slip conditions and comparing with three-dimensional calculations we have explored the question whether the MDR is applicable for the simulation of bi-axial in-plane loadings. We have found that the corresponding mapping is not exact (there are local violations of stick and slip conditions) but has an acceptable accuracy comparable with the accuracy of the Cattaneo and Mindlin solution for tangential contact. Comparison with three-dimensional simulations shows a good qualitative agreement but some quantitative deviations. We have found that the dependencies of the dissipated energy on the amplitude of loading, obtained for various values of R_M , fit into one universal curve. This curve may be approximated by a power law in the range of small values of $Q/\mu F_z < 0.7$. The obtained results may be helpful for a better understanding of the mechanics of tangential contacts under bi-axial loading.

Acknowledgements: A.V. Dimaki is thankful for the funding of the Fundamental Research Program of the State Academies of Sciences for 2013–2020. R. Pohrt and V.L. Popov thank V. Aleshin for helpful discussions.

REFERENCES

1. Dimaki, A.V., Dmitriev, A.I., Chai, Y.S., Popov, V.L., 2014, *Rapid simulation procedure for fretting wear on the basis of the method of dimensionality reduction*, Int. J. Solids and Struct., 51, pp. 4215–4220.
2. Ginsberg, J.H., 2001, *Mechanical and Structural Vibrations: Theory and Applications*. Wiley, 704 p.
3. Cattaneo C., 1938, *Sul contatto di due corpi elastici: distribuzione locale degli sforzi*, Rendiconti dell'Accademia nazionale dei Lincei, 27, 342–348, 434–436, 474–478.
4. Mindlin, R.D., Mason, W.P., Osmer, T.F., Deresiewicz, H., 1951, *Effects of an oscillating tangential force on the contact surfaces of elastic spheres*, Proc. First US National Congress of Appl. Mech., pp. 203–208.
5. Popov, V.L., Heß, M., 2015, *Method of Dimensionality Reduction in Contact Mechanics and Friction*, Berlin, Heidelberg: Springer, 265 p.
6. Popov, V.L., 2017, *Contact Mechanics and Friction. Physical Principles and Applications*, 2nd Edition, Berlin, Heidelberg: Springer, 391 p.
7. Johnson, K.L., 1955, *Surface interaction between elastically loaded bodies under tangential forces*, Proceedings of the Royal Society, A230, p. 531–548.
8. Munisamy, R.L., Hills D.A., Nowell D., 1994, *Static Axisymmetric Hertzian Contacts Subject to Shearing Forces*, ASME Journal of Applied Mechanics, 61, pp. 278–283.
9. Gallego, L., Nelias, D., and Deyber, S., 2010, *A fast and efficient contact algorithm for fretting problems applied to fretting modes I, II and III*, Wear, 268.1, pp. 208–222.
10. Ciavarella, M., 2013, *Frictional energy dissipation in Hertzian contact under biaxial tangential harmonically varying loads*, J. Strain Analysis, 49(1), pp. 27–32.
11. Popov, V.L., Hess, M., 2014, *Method of dimensionality reduction in contact mechanics and friction: a user's handbook. I. Axially-symmetric contacts*, Facta Univ. Mech. Engng. 12, pp. 1–14.
12. Johnson, K.L., 1985, *Contact mechanics*, Cambridge: Cambridge University Press, 452 p.